Pauli-blocking effects and Cooper triples in three-component Fermi gases

P. Niemann[*] and H.-W. Hammer[†]

Helmholtz-Institut für Strahlen- und Kernphysik (Theorie) and Bethe Center for Theoretical Physics,
Universität Bonn, 53115 Bonn, Germany

We investigate the effect of Pauli blocking on universal two- and three-body states in the medium. Their corresponding energies are extracted from the poles of two- and three-body in-medium scattering amplitudes. Compared to the vacuum, the binding of dimer and trimer states is reduced by the medium effects. In two-body scattering, the well-known physics of Cooper pairs is recovered. In the three-body sector, we find a class of positive energy poles which can be interpreted as Cooper triples.

I. INTRODUCTION

Ultracold Fermi gases offer a unique possibility to investigate many-body phenomena in a controlled environment [1–4]. In dilute systems of two-component fermions, the interactions are characterized by the *S*-wave scattering length. Close to a Feshbach resonance, the scattering length can be tuned experimentally by varying an external magnetic field. In particular, the crossover from the Bardeen-Cooper-Schrieffer (BCS) limit of weakly interacting fermions to a Bose-Einstein condensation (BEC) of bosonic dimers by tuning through a resonance has been studied in great detail [4]. The behavior of such a system is constrained by universal relations that involve the so-called contact, which measures the number of pairs of fermions with different spins that have small separations [5,6].

More recently, ultracold gases of three-component fermions have also been investigated. The interest in such systems has various motivations. First, the manifestation of the Efimov effect [7] has been studied in systems consisting of three hyperfine states of fermionic ^{6}Li atoms. A resonant enhancement of the recombination rates at certain values of the scattering lengths was observed in experiment [8,9]. These observations were analyzed theoretically and traced back to the appearance of an Efimov trimer close to the three-atom threshold [10–13]. Subsequently, the direct association of Efimov trimers was also achieved [14,15].

A second line of research has focused on the phase structure of such systems [16–19]. In these theoretical studies, two components are typically paired while the third one remains unpaired. This mechanism can be regarded as a generalization of the BCS case. Moreover, the BEC-BCS crossover has also been investigated in a three-component system. In Ref. [20], the dynamics of such a system was analyzed on time scales long enough to see two-body physics but short enough to be able to neglect Efimov states or three-body collisions. For three-component fermions in an optical lattice, the formation of a superfluid phase at weak coupling and a "trion" phase of three-fermion bound states at strong coupling has been predicted [21].

In this work, we combine both lines of research and investigate three-body correlations in the medium. We investigate the effect of Pauli blocking induced by the presence of a Fermi sphere on universal two- and three-body states in the medium. Their corresponding energies are extracted from the poles of two- and three-body scattering amplitudes in the medium. A similar study was carried out in Ref. [22] for the case of a fermion immersed in a Fermi sea interacting with two heavy bosons. The Born-Oppenheimer approximation was used to map the system to an effective two-body problem and calculate the dependence of the universal spectrum of Efimov trimers on the Fermi density in that case. In Ref. [23], the modification of the Efimov spectrum for three equal-mass fermions when one of the fermions is embedded in a Fermi sea was calculated numerically and the modification of the universal scaling behavior by the background density of fermionic particles was investigated.

Here, we investigate the medium modifications for three equal-mass fermions, all of which are embedded in a Fermi sphere. We solve the two- and three-body scattering equations for this system (cf. Ref. [10]) in the medium and present a detailed study of the poles of the in-medium scattering amplitude. In particular, we study the emergence of positive-energy three-body poles analogous to the Cooper pairs in the two-body system. A similar analysis was carried out in Refs. [24] for the in-medium scattering amplitude of a boson and a fermion. In these studies, the boson-fermion Cooper pairs were found to persist for vanishing attraction.

We consider three distinguishable nonrelativistic particles of equal mass with resonant interactions in a Fermi sea at zero temperature. The system is assumed to be dilute, i.e., $k_F R \ll 1$, where R is the range of the interaction and k_F the Fermi momentum. In this case, the two-body interactions of the particles are determined by their scattering length a. We assume the two-body interactions to be resonant, i.e., $|a| \gg R$. Effective range corrections are suppressed and can be treated in perturbation theory. Because we are at zero temperature, all states up to k_F are occupied. For $k_F a \ll 1$, a perturbative low-density expansion can be derived [25], but for $k_F a \sim 1$ an infinite class of diagrams has to be resummed and one has to resort to Monte Carlo simulations or additional expansions [3,26]. In this study, we include only the interaction of the particles with the Fermi sea via Pauli blocking. These effects dominate in an expansion in the inverse number of dimensions [27,28] and determine the qualitative behavior of the system. Other effects of the medium, such as the excitation of particles out of the Fermi sea through scattering processes, are neglected.

---
[*]niemann@hiskp.uni-bonn.de
[†]hammer@hiskp.uni-bonn.de

Our theoretical framework is based on an effective Lagrangian for the fermion fields Ψ_i, $i = 0,1,2$:

$$\mathcal{L} = \sum_{i=0}^{2} \Psi_i^\dagger \left(i\partial_t + \frac{\vec{\nabla}^2}{2m} \right) \Psi_i - \sum_{k=0}^{2} \frac{g_k}{2} \Psi_i^\dagger \Psi_j^\dagger \Psi_i \Psi_j$$
$$+ h\, \Psi_0^\dagger \Psi_1^\dagger \Psi_2^\dagger \Psi_0 \Psi_1 \Psi_2, \tag{1}$$

where the coupling constant g_k with $i \neq j \neq k$ parametrizes the interaction of fermions i and j. The term proportional to h is a contact three-body interaction of all three fermions. It determines the spectrum of three-body Efimov states in the vacuum. The explicit form of this term will not be required for our study, since the dependence on the three-body term can be traded for a dependence on the cutoff in leading-order calculations [29]. For practical calculations, it is convenient to introduce auxiliary dimer fields d_k and rewrite the Lagrangian in the form

$$\mathcal{L} = \sum_{i=0}^{2} \Psi_i^\dagger \left(i\partial_t + \frac{\vec{\nabla}^2}{2m} \right) \Psi_i + \sum_{k=0}^{2} \left[\Delta_k d_k^\dagger d_k \right.$$
$$\left. - \frac{g_k}{2} (d_k^\dagger \Psi_i \Psi_j + \Psi_i^\dagger \Psi_j^\dagger d_k) \right] + h\, \Psi_0^\dagger \Psi_1^\dagger \Psi_2^\dagger \Psi_0 \Psi_1 \Psi_2. \tag{2}$$

The dimer field d_k describes two interacting particles i and j with $i \neq j \neq k$. Using the classical equations of motion, the equivalence of Eqs. (1) and (2) can be demonstrated. This framework has been widely used to describe the universal properties of few-body systems close to the universal limit [30]. It has also been used as the basis for studies of the Efimov effect in systems three-component fermions [10,13].

II. TWO-BODY SECTOR

A. Vacuum case

We are now in the position to investigate the effect of Pauli blocking on universal two- and three-body states in the medium. We start by briefly reviewing the vacuum case. More details can be found in Ref. [30]. For convenience, we set $\hbar = m = 1$ from now on. The bare dimer propagator derived from the Lagrangian (2) is simply a constant, i/Δ_k. The full, interacting dimer propagator is given by dressing the bare propagator with fermion bubbles; see Fig. 1. It represents the exact solution of the vacuum two-body problem for the Lagrangian (2). The diagrams constitute a geometric series, which can easily be summed. The result can be written as

$$iD_k(P_0,\mathbf{P}) = \frac{i}{\Delta_k \left[1 - \frac{g_k^2}{4\Delta_k} I(P_0,\mathbf{P}) \right]}, \tag{3}$$

where $I(P_0,\mathbf{P})$ is the loop function for the two-fermion bubble in Fig. 1. In the vacuum, the loop function is

$$iI(P_0,\mathbf{P}) = \int_{|\mathbf{q}|<\Lambda} \frac{d^4q}{(2\pi)^4} \frac{i}{\frac{P_0}{2} + q_0 - \frac{1}{2}\left(\frac{\mathbf{P}}{2} + \mathbf{q}\right)^2 + i\epsilon}$$
$$\times \frac{i}{\frac{P_0}{2} - q_0 - \frac{1}{2}\left(\frac{\mathbf{P}}{2} - \mathbf{q}\right)^2 + i\epsilon}$$
$$= \frac{i}{4\pi}\left(-\frac{2\Lambda}{\pi} + \sqrt{-P_0 + P^2/4 - i\epsilon} \right), \tag{4}$$

where $P \equiv |\mathbf{P}|$ and the UV divergence of the loop integral has been regulated by a momentum cutoff Λ. The cutoff dependence is absorbed into the coupling constant g_k, such that all observable quantities are independent of Λ. The two-body scattering amplitude is obtained by multiplying the full dimer propagator with the square of the dimer-fermion coupling, $(-ig_k/2)^2$. Matching to the amplitude for scattering of particles i and j in the center of mass at energy $E = p^2$,

$$T_k(p^2) = \frac{4\pi}{-1/a_k - ip} \overset{!}{=} -\frac{g_k^2}{4} D_k(p^2,0), \tag{5}$$

we obtain

$$\frac{g_k^2}{\Delta_k} = \frac{16\pi a_k}{1 - 2a_k\Lambda/\pi}. \tag{6}$$

Note that g_k and Δ_k are not independent at this order and all observables depend on the combination g_k^2/Δ_k. The renormalized dimer propagator in the vacuum thus can be written as

$$iD_k(P_0,\mathbf{P})_{vak} = i\frac{16\pi}{g_k^2}[1/a_k - \sqrt{-P_0 + P^2/4 - i\epsilon}]^{-1}. \tag{7}$$

The propagator has a bound state pole at $P_0 = -1/a_k^2 + P^2/4$ if $a_k > 0$. The energy at the pole is composed of the binding energy $-1/a_k^2$ and the kinetic energy of the dimer $P^2/4$. The total mass is $2m = 2$, as expected for a dimer state. For negative scattering length, the pole is on the unphysical sheet and represents a virtual state.

B. Medium case

We now move on to medium case. In the presence of a Fermi sphere, the loop integral changes to

$$iI(P_0,\mathbf{P}) = \int_{|\mathbf{q}|<\Lambda} \frac{d^4q}{(2\pi)^4} \frac{i\Theta\left(\left|\frac{\mathbf{P}}{2} + \mathbf{q}\right| - k_F\right)}{\frac{P_0}{2} + q_0 - \frac{1}{2}\left(\frac{\mathbf{P}}{2} + \mathbf{q}\right)^2 + i\epsilon}$$
$$\times \frac{i\Theta\left(\left|\frac{\mathbf{P}}{2} - \mathbf{q}\right| - k_F\right)}{\frac{P_0}{2} - q_0 - \frac{1}{2}\left(\frac{\mathbf{P}}{2} - \mathbf{q}\right)^2 + i\epsilon}, \tag{8}$$

where the θ functions encode the Pauli blocking. They ensure that the intermediate particles cannot scatter into occupied states in the Fermi sea. This introduces boundary conditions for the loop integrals at small momenta. Different cases must
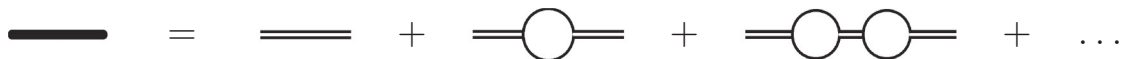

FIG. 1. Bubble sum for the full interacting dimer propagator (thick line). The double lines correspond to the bare dimer propagator and the single lines indicate particle propagators.

be considered. A summary of the calculation is given in Appendix A. Here we focus on the results.

For vanishing total momentum P the boundary conditions become simple. In this case, the argument of both θ functions is $|\mathbf{q}| - k_F$. Consequently, the integration over $|\mathbf{q}|$ starts at k_F and ends at Λ. It is evident that only the infrared behavior of the integrals is modified by the Fermi sea. The renormalization of UV divergences is the same as in the vacuum. The in-medium dimer propagator then has the form

$$i D_k(P_0, P) = i \frac{16\pi}{g_k^2} \left[\frac{1}{a_k} - \frac{1}{\pi} L(P_0, P) \right]^{-1}, \qquad (9)$$

with

$$L(P_0, P = 0) = 2k_F + \sqrt{P_0 + i\epsilon}[\ln(k_F - \sqrt{P_0 + i\epsilon}) \\ - \ln(k_F + \sqrt{P_0 + i\epsilon})]. \qquad (10)$$

The poles of the propagator are determined by solving

$$\frac{1}{a_k} = \frac{2k_F}{\pi} + \frac{\sqrt{P_0 + i\epsilon}}{\pi}[\ln(k_F - \sqrt{P_0 + i\epsilon}) \\ - \ln(k_F + \sqrt{P_0 + i\epsilon})] \qquad (11)$$

for P_0. If P_0 is negative, this equation can be written as

$$\frac{1}{a_k} = \frac{2k_F}{\pi} + \frac{2}{\pi}\sqrt{|P_0|} \arctan\left(\frac{\sqrt{|P_0|}}{k_F}\right), \qquad (12)$$

where the $i\epsilon$ has been omitted. This equation is formally similar to Eq. (3) of Ref. [22] for the binding energy of a light fermion immersed in a Fermi sea interacting with two heavy bosons. In this case, the Born-Oppenheimer approximation may be used and the three-body problem reduces to an effective two-body problem.

In the general case, the boundary conditions are more complex (cf. Appendix A). Two cases have to be distinguished: $P < 2k_F$ and $P > 2k_F$. The result for the general in-medium loop function $L(P_0, P)$ is

(a) $P < 2k_F$:

$$L(P_0, P) \\ = P/2 + k_F + \sqrt{\sigma}[\ln(P/2 + k_F - \sqrt{\sigma}) \\ - \ln(P/2 + k_F + \sqrt{\sigma})] + \frac{k_F^2 - P_0 - i\epsilon}{P} \\ \times \left[\ln(P/2 + k_F - \sqrt{\sigma}) + \ln(P/2 + k_F + \sqrt{\sigma}) \\ - \ln\left(\sqrt{k_F^2 - \frac{1}{4}P^2} - \sqrt{\sigma}\right) - \ln\left(\sqrt{k_F^2 - \frac{1}{4}P^2} + \sqrt{\sigma}\right) \right], \qquad (13)$$

(b) $P > 2k_F$:

$$L(P_0, P) \\ = 2k_F + \pi\sqrt{-\sigma} + \sqrt{\sigma}[\ln(P/2 - k_F + \sqrt{\sigma}) \\ + \ln(P/2 + k_F - \sqrt{\sigma}) - \ln(P/2 - k_F - \sqrt{\sigma}) \\ - \ln(P/2 + k_F + \sqrt{\sigma})] + \frac{-k_F^2 + P_0 + i\epsilon}{P} \\ \times [\ln(P/2 - k_F - \sqrt{\sigma}) + \ln(P/2 - k_F + \sqrt{\sigma}) \\ - \ln(P/2 + k_F - \sqrt{\sigma}) - \ln(P/2 + k_F + \sqrt{\sigma})], \qquad (14)$$

with $\sqrt{\sigma} = \sqrt{P_0 - P^2/4 + i\epsilon}$.

We now discuss the poles of the dimer propagator in the medium. Our aim is to recover the known two-body physics from the viewpoint of the pole structure and then use the same strategy to understand the three-body sector. First, we specify our units. Since there is one free length scale l_0 in the calculations, we express all dimensionful quantities in units of l_0: the energy has the unit $[1/l_0^2]$, scattering lengths $[l_0]$, and momenta $[1/l_0]$.

We never find more than one pole on the physical sheet in the in-medium dimer propagator. The physical conditions under which this pole can disappear are discussed below. In Fig. 2, the energy of the pole, E, is plotted against the inverse scattering length $1/a_k$ at vanishing momentum $P = 0$ for $k_F l_0 = 0.7$ (solid line) and 1 (dash-dotted line), respectively. The dashed curve represents the dimer energy in the vacuum case. For positive scattering length, the energy of the vacuum pole is $E = -1/a_k^2$. There is no vacuum pole on the physical sheet if the scattering length is negative. For nonvanishing Fermi momentum, a pole with positive energy appears in the negative-scattering-length region. In the limit $1/a_k \rightarrow -\infty$, this pole asymptotically approaches the values $(k_F l_0)^2 = 0.49$ and 1 for $k_F l_0 = 0.7$ and 1, respectively. In the positive-scattering-length region, the pole behaves like a vacuum pole if the scattering length is sufficiently small. However, the corresponding binding energy is reduced by medium effects. Additionally, four selected points are marked on the solid line: I, II, III, and IV. To gain deeper insight into the nature of the pole in the in-medium dimer propagator, these points will be further investigated below. The parameters k_F and a are kept fixed while the momentum P will be varied.

In the inset of Fig. 2, which corresponds to point I, the dependence of the pole energy on the total momentum P is shown for $a_k = l_0$ and $k_F = 0.7/l_0$ (solid line). The dashed line shows the vacuum pole energy as before. Medium and vacuum poles have a similar behavior as function of the total
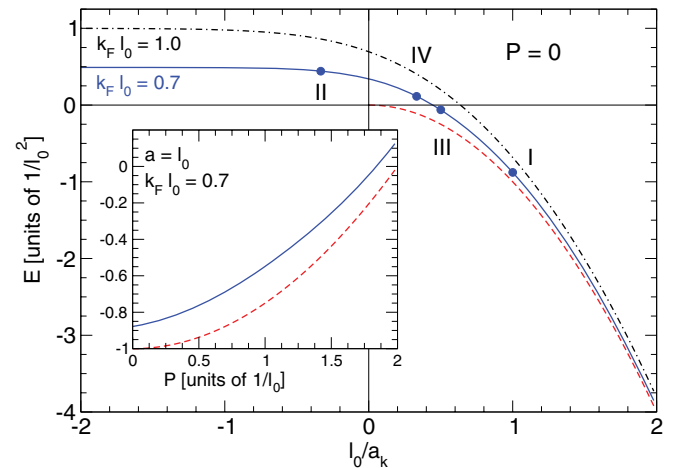

FIG. 2. (Color online) The energy E of the dimer pole at $P = 0$ plotted against the inverse scattering length $1/a_k$ for a Fermi momentum $k_F = 0.7/l_0$ (solid line) and $k_F = 1/l_0$ (dash-dotted line). In addition, four selected points are marked I, II, III, and IV on the solid line. For comparison, the vacuum pole energy is shown by the dashed line. In the inset, the dimer pole energy is displayed as a function of the total momentum P for $k_F = 0.7/l_0$ and $a = l_0$. Curves are as above.
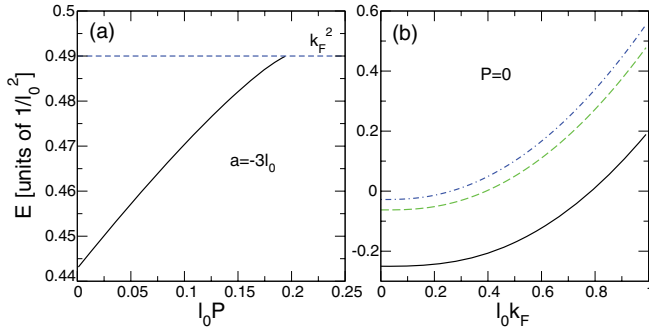
FIG. 3. (Color online) (a) The energy E depicted as function of the total momentum P for $a_k = -3l_0$ and $k_F = 0.7/l_0$ (solid line). The vertical dotted line gives $E = k_F^2$. (b) Energy E plotted against the Fermi momentum k_F for $a_k = 2l_0$ (solid), $4l_0$ (dashed), $6l_0$ (dashed dotted); $P = 0$.
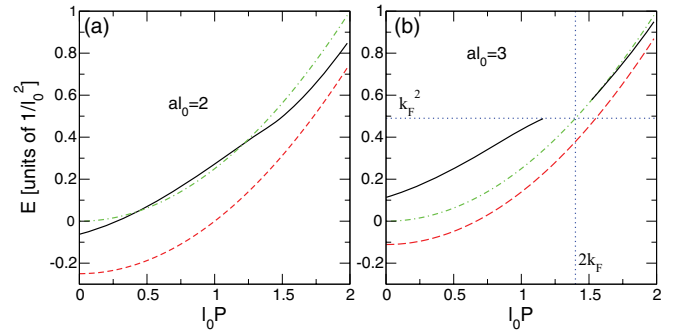

FIG. 4. (Color online) The energy of the poles plotted as a function of the total momentum P for $a = 2l_0$ [panel (a)] and $a = 3l_0$ [panel (b)] and $k_F = 0.7l_0$ (solid line). The dashed line shows the vacuum poles and the dash-dotted line gives the kinetic energy $P^2/4$. The horizontal dotted line in (b) gives k_F^2 and the vertical dotted line gives $2k_F$.

momentum: with increasing momentum P, the pole energy is increased and the binding is reduced. For the vacuum pole, this is evident from Eq. (7). In the medium, it follows from the dominant functional dependence of the in-medium dimer propagator on $\sigma = P_0 - P^2/4$ [cf. Eqs. (13) and (14)]. Moreover, medium effects are again seen to lower the pole energies.

Next, we examine the positive energy poles more thoroughly. In Fig. 3(a), the energy is plotted against the total momentum for a negative scattering length $a_k = -3l_0$, which corresponds to point II in Fig. 2. The energy of the pole is positive and continuously rises as the momentum P is increased until the energy reaches the value $k_F^2 = 0.49/l_0^2$, where the pole disappears. This positive energy pole can be associated with Cooper pairs [31]. With this interpretation, their peculiar behavior can be understood. Assume that the two particles are inside the Fermi sphere. If there is no interaction, the energy of the particles is just their kinetic energy. In the presence of attractive interactions, the energy of the two particles, given by the pole energy, is lowered. Consequently, the energy gain ΔE is the difference of the kinetic energy and the pole energy. Because the maximum kinetic energy of two particles inside the Fermi sea is $k_F^2/2 + k_F^2/2$, the maximum energy of the pole is also k_F^2. When the total momentum of the two particles becomes too large, the pole disappears. This property is compatible with the intepretation as Cooper pairs, whose total momentum is commonly assumed to be zero. Remember that the energy threshold already appeared in Fig. 2. But in this instance a different limit was considered. The energy of the pole approaches the threshold k_F^2 asymptotically in the limit $1/a_k \to -\infty$. The energy gain ΔE, hence, decreases in this limit. But the poles never disappear and Cooper pairs can always be formed in this region.

We now turn to the dependence of the poles on the Fermi momentum in the positive-scattering-length region. In Fig. 3(b), the pole energy is plotted against the Fermi momentum. The total momentum P is set to zero and the scattering lengths are $a_k = 2l_0$, $4l_0$, and $6l_0$. As expected, the energy is negative at $k_F = 0$ and the pole corresponds to a bound state. With increasing Fermi momentum, the medium effects become stronger and the binding is reduced. For small k_F the energy rises only slowly but at larger Fermi momentum

the energy changes rapidly, crosses zero, and becomes positive. Hence, we observe a continuous crossover from bound states to positive energy poles as the Fermi momentum is increased.

So far, we could associate the left and right regions in Fig. 2 to Cooper pairs (cf. II) and bound states (cf. I), respectively. In between lies the crossover region. We will investigate this region further at the two remaining points, III and IV. Here the nature of the poles changes as a function of momentum.

In Fig. 4(a) the energy of the pole is plotted against the total momentum (solid line) with $a = 2l_0$ corresponding to point III in Fig. 2. By comparision, the dashed line shows the vacuum pole and the dash-dotted line the kinetic energy $P^2/4$. For vanishing momentum the energy of the pole is extremely reduced compared to the vacuum but still negative. However, in the region around $P = l_0$ the energy becomes bigger than the kinetic energy. Hence, this pole cannot correspond to a bound state in this region. For larger momenta the energy again drops below the kinetic energy and the poles behave similarily to vacuum poles.

We now turn to point IV in the crossover region. In Fig. 4(b) an entirely different behavior can be observed. Again, the vacuum pole (dashed line) and the kinetic energy (dash-dotted line) are shown. Striking are the three qualitatively different regions in this graph. For momenta $P < 2k_F$ the pole seems to correspond to a Cooper pair: At $P = 0$ the energy of the poles is positive, and in this whole region the energy is larger than the kinetic energy, and the pole disappears when the energy approaches k_F^2. In a region around $P \approx 2k_F$ there is no pole at all. For slightly larger momenta, the pole reappears. At first the energy is very close to the kinetic energy, but for larger momentum it approaches the vacuum energy, as expected. These poles now behave like a bound state.

In summary, we have related the positive-energy poles at $P = 0$ to Cooper pairs and the negative-energy poles to bound states. A finite momentum P leads to an increase in the pole energy. In the vacuum, the additional energy is simply the kinetic energy $P^2/4$. In the medium, the pole energy also increases but the dependence on P is more complicated. In particular, the poles can vanish and change their character.

As the Fermi momentum k_F is increased, e.g., the binding energy is reduced by medium effects. We identified the two extremes I and II in Fig. 2 with the BCS and BEC domains, respectively. In between there is a crossover region. In this region the poles change their character as a function of the momentum P and they cannot be uniquely related to one of the two cases. Equipped with this qualitative understanding of in-medium two-body physics, we move on to the three-body amplitude.

III. THREE-BODY SECTOR

A. Vacuum case

We start by briefly reviewing the physics issues of the vacuum case and then move on to the medium. In the three-body system with resonant interactions, there is a universal spectrum of three-body bound states with an accumulation point at zero energy, called Efimov states [7]. The spectrum is given by Efimov's universal equation

$$E_B^{(n)} + \frac{1}{a^2} = (e^{-2\pi/s_0})^{n-n_*} \exp[\Delta(\xi)/s_0]\kappa_*^2, \qquad (15)$$

where the angle ξ is defined by

$$\tan\xi = -a\sqrt{E_B^{(n)}}, \qquad (16)$$

$s_0 \approx 1.00624$ is a transcendental number, and κ_* is the binding wave number of the state labeled n_*. The function $\Delta(\xi)$ was first calculated in Ref. [32] and satisfies $\Delta(-\frac{1}{2}\pi) = 0$. In the unitary limit of infinite scattering length, the spectrum thus becomes geometric. The qualitative features of this spectrum are determined by the scattering length a, but the exact energies depend on the three-body interaction in Eq. (2) which fixes the value of κ_* [33]. The spectrum exhibits a discrete scaling symmetry which is evident in Eq. (15): if the scattering length a and the energies E_B are rescaled by the discrete scaling factor $\lambda = \exp(\pi/s_0)$ and λ^{-2}, respectively, but κ_* remains fixed the spectrum is mapped onto itself. If the scattering length dependence of one state is known, all others thus can be obtained from the scaling transformation. A detailed discussion of these issues can be found in Ref. [30]. Here, we focus on the modification of this spectrum in the medium and on possible positive energy poles in the three-body amplitude similarly to the two-body case discussed above. As discussed above, we set the three-body interaction to zero in our calculation. Thus, κ_* is proportional to the momentum cutoff Λ. The exact proportionality factor is not required for our purpose. A detailed study of the Efimov spectrum and the universal scaling relations in the presence of one Fermi sphere was carried out in Ref. [23]. We go beyond this study by considering three Fermi spheres and explicitly focusing on the emergence positive energy poles in the three-body amplitude. Preliminary results of our study were already presented in Ref. [34].

B. Medium case

The three-particle scattering amplitude in the medium can be calculated by solving an integral equation. In order to simplify the boundary conditions given by the Pauli blocking, we will constrain the total momentum of the three particles to
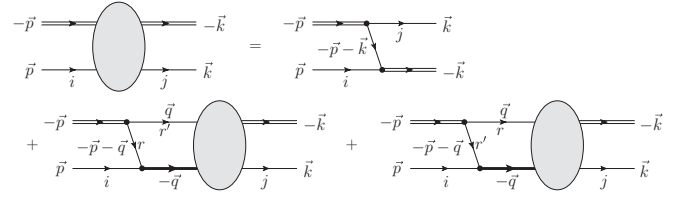

FIG. 5. Feynman diagrams for the fermion-dimer scattering amplitude for zero total momentum. Momenta **p**, **q**, **k** and fermion indices i,j,r,r' are assigned as in Eq. (17).

be zero. We note that the Fermi sea provides a special reference frame and a nonzero momentum cannot be obtained from a simple Galilei transformation. However, we have seen in the two-body case that a nonzero momentum essentially increases the pole energy. Outside of the crossover region, the qualitative behavior remains unchanged (cf. inset of Fig. 2). We expect the same to be true in the three-body case. The Feynman diagrams for the three-body scattering amplitude are depicted in Fig. 5. Since we are interested in the three-body singularities of the amplitude, it is sufficient to consider the fermion-dimer scattering amplitude where the external dimer propagators are amputated. Because the three particles are distinguishable, we have one inhomogeneous and two homogeneous contributions to the amplitude as the intermediate dimer can be formed in two ways [10]. The integral equation for the amplitude $\mathcal{A}_{ij}$ can be written as

$$i\mathcal{A}_{ij}(\mathbf{p},\mathbf{k},E,E_i,E_j)$$
$$= -\frac{g_i g_j}{4} \frac{i\Theta(|\mathbf{p}+\mathbf{k}|-k_F)}{E - E_i - E_j - \frac{(\mathbf{p}+\mathbf{k})^2}{2} + i\epsilon}(1-\delta_{ij})$$
$$+ \sum_{r=0}^{2}\left(-\frac{g_i g_r}{4}\right)\int_{|\mathbf{q}|<\Lambda}\frac{d^4 q}{(2\pi)^4}\frac{i\theta(q-k_F)}{q_0 - \frac{1}{2}q^2 + i\epsilon}$$
$$\times \frac{i\theta(|\mathbf{p}+\mathbf{q}|-k_F)}{E - E_i - q_0 - \frac{1}{2}(\mathbf{p}+\mathbf{q})^2 + i\epsilon}$$
$$\times i D_r(E-q_0,q)(1-\delta_{ir})i\mathcal{A}_{rj}(\mathbf{q},\mathbf{k},E,q_0,E_j), \qquad (17)$$

where the momenta and particle indices are assigned as in Fig. 5 and E is the total energy. After setting the energies of the incoming and outgoing particles, E_i and E_j, on shell, the bare coupling constants are removed by defining a renormalized amplitude,

$$\mathcal{A}_{ij}^R(\mathbf{p},\mathbf{k},E) = \sqrt{|Z_i||Z_j|}\mathcal{A}_{ij}(\mathbf{p},\mathbf{k},E), \qquad (18)$$

where Z_i is the residue of the dimer pole i in the vacuum,

$$Z_i = \frac{32\pi}{g_i^2 a_i}. \qquad (19)$$

This renormalized amplitude has the same poles in the three-body sector as the three-particle scattering amplitude. We now expand the fermion-dimer amplitude in partial waves as

$$\mathcal{A}_{ij}^R(\mathbf{p},\mathbf{k},E) = \sum_{l=0}^{\infty}(2l+1)\left(\mathcal{A}_{ij}^R\right)_l[p,k,E]P_l(\cos\theta_k), \qquad (20)$$

where $\cos\theta_k = \mathbf{p}\cdot\mathbf{k}/(pk)$ and P_l is a Legendre polynomial. The different partial waves decouple and the integral equation

for the lth partial wave amplitudes is

$$
\begin{aligned}
i\big(\mathcal{A}_{ij}^R\big)_l[p,k,E] \\
= \frac{1}{2} \frac{-8\pi i}{\sqrt{|a_i||a_j|}} \int_{-1}^{1} d\cos\theta_k \, P_l(\cos\theta_k) \, t_{ij}(p,k,\theta_k,E) \\
+ i \sum_{r=0}^{2} 4\pi \frac{\sqrt{|a_r|}}{\sqrt{|a_i|}} \int_{k_F}^{\Lambda} \frac{dq}{(2\pi)^2} q^2 \int_{-1}^{1} d\cos\theta_q \, P_l(\cos\theta_q) \\
\times t_{ir}(p,q,\theta_q,E) \, \overline{D}_r(q,E)\big(\mathcal{A}_{rj}^R\big)_l[q,k,E],
\end{aligned}
\tag{21}
$$

where

$$
t_{ij}(p,k,\theta_k,E) := \frac{\theta(|\mathbf{p}+\mathbf{k}|-k_F)(1-\delta_{ij})}{E-p^2-k^2-pk\cos\theta_k+i\epsilon}
\tag{22}
$$

and

$$
\overline{D}_r(q,E) := \left[\frac{1}{a_r} - \frac{1}{\pi}L\left(E - \frac{1}{2}q^2,q\right)\right]^{-1}
\tag{23}
$$

is the dimer propagator without prefactors. In the vacuum only the S-wave amplitude has bound state poles. This remains true in the medium and we, thus, focus on the poles of the S-wave in-medium amplitude $(\mathcal{A}_{ij}^R)_0[p,k,E]$. The technical details of the implementation of the boundary conditions from the Pauli blocking are discussed in Appendix A. In the next section, we present our results for the pole structure of $(\mathcal{A}_{ij}^R)_0[p,k,E]$.

C. Results

In this section we discuss the poles of the the S-wave amplitude $(\mathcal{A}_{ij}^R)_0$, in general, for three different scattering lengths. In Eq. (21) the three-body force dependence was traded for the cutoff dependence, so the cutoff determines the three-body energy in the vacuum for given scattering lengths. A spectrum of two states as a function of the Fermi momentum is shown in Fig. 6. Similarly to the two-body case, the binding energy of each state decreases with rising Fermi momentum due to medium effects. The difference of the energy loss with increasing Fermi momentum for shallow and deep states is remarkable. The less bound state disappears through the threshold while the more deeply bound state loses only about 5% of its binding energy as $k_F l_0$ is increased from 0 to 1. This
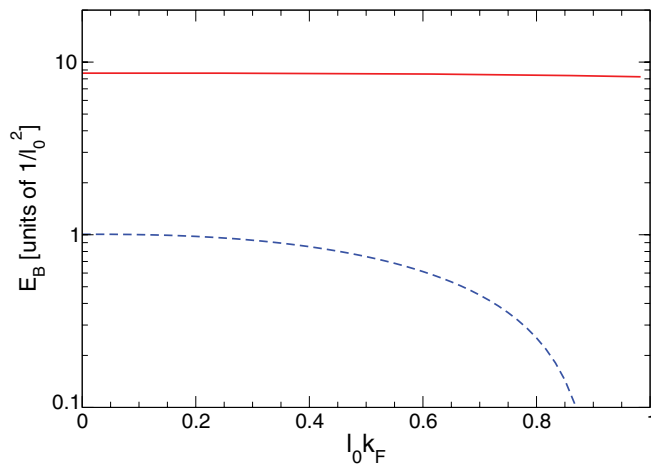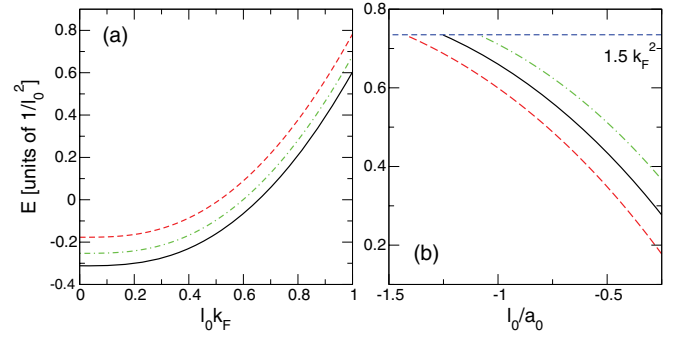
FIG. 7. (Color online) (a) Energy of three-body poles plotted against k_F for $a_0 = -1.0 l_0$ (dashed), $a_0 = -1.25 l_0$ (dash-dotted), and $a_0 = -1.5 l_0$ (solid); $\Lambda = 150/l_0$ and the remaining scattering lengths are $a_1 = -2 l_0$ and $a_2 = -2.5 l_0$. (b) The pole energy is shown as a function of $1/a_0$ for $\Lambda = 150/l_0$ (dash-dotted), $\Lambda = 160/l_0$ (solid), and $\Lambda = 170/l_0$ (dashed); $k_F = 0.7/l_0$ and the remaining scattering lengths are $a_1 = -l_0$ and $a_2 = -0.99 l_0$. The horizontal line gives $E = 1.5 k_F^2$.

behavior of the three-body spectra is generic and was always observed in our calculations.

In Fig. 7(a) the energy of a generic three-body pole is plotted against the Fermi momentum for three negative scattering lengths. As in the previous case, the binding energy reduces with increasing Fermi momentum. Indeed, the energy goes to zero and continuously rises to positive values. Hence, we have found poles with positive energy. Since the total momentum is zero, they cannot correspond to bound states. Note the resemblance between this figure and Fig. 3, which shows dimer poles.

To get a better understanding of these positive energy poles, we have varied one of the three negative scattering lengths while keeping the other two constant; see Fig. 7(b). The energy rises with decreasing $1/a$ but vanishes when the value of the energy becomes $1.5 k_F^2$. For different configurations of the Fermi momenta, scattering lengths, and the cutoff, we have always found this threshold. The accuracy of the location of this threshold reaches to the third (fourth) decimal place for cutoffs of the order 100 (10) l_0. In order to explain this observation, we draw an analogy with the positive energy poles in the two-body case. There, the energy gain ΔE is the kinetic energy minus the energy of the pole. Hence, the energy of the pole cannot be larger than the maximum kinetic energy. In Fig. 8 configurations of two and three particles inside the Fermi sphere are shown for total momentum $P = 0$. As discussed in the previous section, the maximum two-body pole energy

FIG. 6. (Color online) Binding energy E_B of two states depicted in dependence of k_F: $a_k = l_0$ for $k = 0, 1, 2$, and $\Lambda = 250/l_0$.
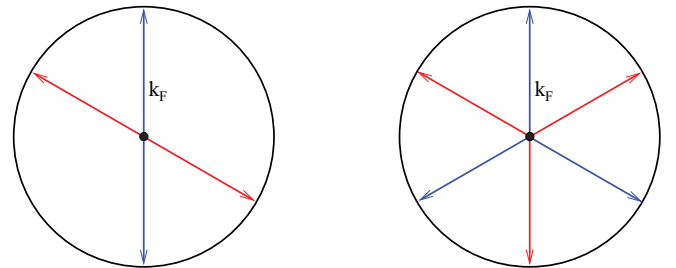
FIG. 8. (Color online) Configurations in the Fermi sphere for two (left) and three particles (right) with total momentum $P = 0$.
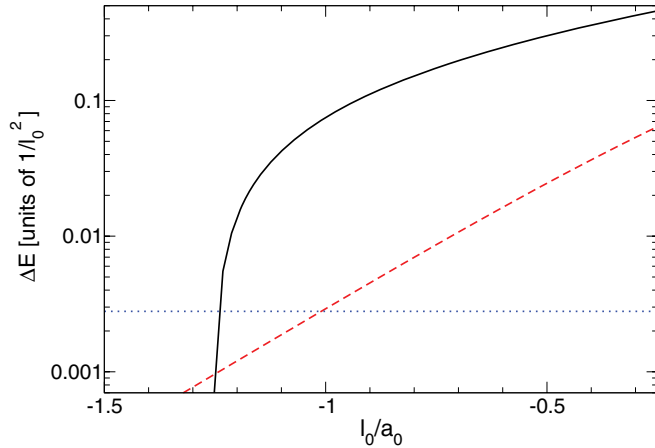
FIG. 9. (Color online) ΔE is plotted against the inverse scattering length $1/a_0$ of three-body (solid line) and two-body (dashed line) poles; $\Lambda = 160/l_0$, $k_F = 0.7/l_0$ and the constant scattering lengths are $a_1 = -l_0$ and $a_2 = -0.99l_0$. The horizontal dotted line shows ΔE for the constant scattering length $a_2 = -0.99l_0$.

is k_F^2. In the case of three particles the magnitude of each momentum can be k_F, whereas the total momentum remains zero. So the maximum kinetic energy of three particles inside the Fermi sphere is $3 \times k_F^2/2 = 1.5k_F^2$. We hypothesize that the three-particle poles belong to a state similiar to a Cooper pair, but built out of three particles, which we call a "Cooper triple." In contrast to Cooper pairs, these Cooper triples are fermions. If the three pair scattering lengths are equal, the Cooper triples are SU(3) singlets. However, for different scattering lengths, the SU(3) symmetry is broken.

Cooper triples also appear if one scattering length is positive. Since the energy of the triples is continuous in $1/a_i$ ($i = 0,1,2$), the region of three negative scattering lengths merges into the region of one positive and two negative scattering lengths at the point $1/a_i = 0$ (the other two scattering lengths are considered constant). Therefore, the pole energy has to remain positive in the limit $1/a_i \rightarrow 0^-$ to obtain Cooper triples for one positive scattering length. For this scenario, the Fermi momentum must be sufficiently large. The actual value depends on the two constant scattering lengths. Hence, Cooper triples also occur in this region. An analogous argument holds if two or three scattering lengths are positive. In all three cases, we have observed Cooper triples in our calculations. However, it remains to be verified that the Fermi spheres assumed in our calculation persist in this region.

Next, we examine which state is energetically favorable. If Cooper pairs are built in a three-component Fermi gas, the pairs are typically formed between two components while the residual component remains unpaired. Therefore, we compare the energy gain of a Cooper triple, $1.5\,k_F^2$ minus pole energy, with the energy gain of a Cooper pair, k_F^2 minus the pole energy. The energy gain ΔE of a Cooper pair and a Cooper triple are compared as a function of one variable scattering length in Fig. 9. The remaining parameters stay the same as in Fig. 7(b). Since ΔE of the Cooper pair depends on the scattering length, it can be energetically favorable to build a different Cooper pair connected to one of the constant scattering lengths. To account for this, we have also plotted the energy gain of the larger

constant scattering length. We find that the energy gain of the three-particle poles is much larger (note the logarithmic axis). The three-particle ΔE rapidly falls off and drops below the energy gain of both Cooper pairs only near the threshold for the triple. This suggests that Cooper triples could play an important role in three-component Fermi gases in the continuum.

In principle, it should always be possible to find these positive energy poles for three negative scattering lengths. In contrast to the two-body case, the poles do not newly emerge in the medium. Primarily, the poles were bound states in the vacuum which became modified by the medium; see Fig. 7(a). Thus, the Fermi momentum must be large enough to obtain positive energy poles. This is most easily achieved for Cooper triples emerging from the rather shallow three-body bound states in vacuum.

IV. CONCLUSION AND OUTLOOK

In this paper, we have examined the influence of Pauli blocking on universal two- and three-body states. First, the poles of the two-body scattering amplitude in the medium were regarded. We were able to recover the physics of Cooper pairs and BEC-BCS crossover from the pole structure of the amplitude. In particular, we found that the binding energy of bound states decreases with rising Fermi momentum due to medium effects. In the negative scattering length region, positive energy poles emerge which can be identified with Cooper pairs. In the crossover region, the poles show a different behavior and their nature changes with the total momentum. They cannot be uniquely identified as bound states or Cooper pairs.

We have used the same strategy to investigate the pole structure of the three-body scattering amplitude. We found that the medium effects reduce the binding of three-body states compared to the vacuum. This is in agreement with the findings of Ref. [23], where the modification of the Efimov spectrum for three equal-mass fermions with one of the fermions embedded in a Fermi sea was calculated. Moreover, we found three-body poles with positive energy. As in the two-body sector, we observed a continuous crossover from negative energy poles to positive energy poles as the Fermi momentum is varied. The maximum energy of the poles was found to be $1.5k_F^2$. In analogy to the connection between positive energy poles in the two-body sector and Cooper pairs, we have interpreted this as evidence for the formation of Cooper triples composed out of three particles. These Cooper triples are fermions and, thus, cannot Bose condense. The energy gain of such a triple was found to be larger than the energy gain of the corresponding Cooper pair over a large region of scattering lengths. Consequently, it appears to be energetically favorable to form a triple instead of a pair and an unpaired third atom in this region. We note that Cooper triples can not form for two-component fermions due to the Pauli principle. The absence of Cooper-type bound states in few-electron systems was demonstrated in [35].

In the case of equal pair scattering lengths, the Cooper triples are SU(3) singlets. For different scattering lengths, however, the SU(3) symmetry is broken (cf. Fig. 7). If the three scattering lengths are large, the SU(3) breaking is small since the leading corrections to the SU(3) limit are proportional to the inverse scattering lengths [36].

How these three-body correlations affect a many-body system is an open question. It would be interesting to extend previous studies of the phase structure of three-component Fermi gases [16–18] to include the triples and investigate their influence. A qualitative picture of the many-body structure in the SU(3) symmetric limit was given by Floerchinger and collaborators [37]. They argue that at small density, if the scattering length is varied from large negative to large positive values, the BCS and BEC phases are separated by a trion phase of three-body bound states. At small densities, our Cooper triples must reduce to the trions of Ref. [37]. A related study for three-component fermions in an optical lattice was carried out in Ref. [21]. Within a Hubbard model with SU(3) symmetry, a trion phase of three-fermion bound states has been predicted at strong coupling and a parallel to the baryonic phase of QCD was drawn.

There may also be a connection to Ref. [24], where boson-fermion (BF) interactions were regarded in a similiar analysis. BF pairs at positive energies were found and the ground state was assumed to be a Fermi gas of BF-Cooper pairs, since the pairs are still fermions. The interaction of three distinguishable fermions in our case could also be regarded as the interaction of a Cooper pair (boson) and a fermion of the remaining type, if the scattering lengths are negative (BCS region) and at least two scattering lengths differ. In this case, we can hypothesize that the ground state of the system is a Fermi gas of Cooper triples, which are composites of a Cooper pair and a unpaired fermion.

Since we have only included the Pauli blocking effects from the medium, further theoretical study is required. This could, for example, be achieved by performing Monte Carlo simulations of such systems similar to the two-flavor case [3]. Such a calculation would allow for more quantitative predictions of the effect. Analogously to Ref. [24], the triples might also lead to a new type of superfluidity in three-component Fermi systems which could be observed in ultracold atomic gases. For this purpose, it would be useful to calculate the interactions of the triples. If their interactions are attractive, they could again form Cooper pairs and Bose condense. Much insight would be gained if one could calculate the energy of such a condensate and compare it with a BCS condensate. This would allow us to determine under which conditions such a new type of superfluidity might occur. An experimental test of this scenario could be carried out with ^{6}Li atoms where mixtures of three different hyperfine states with tunable interactions are already available [8,9,14,15].

ACKNOWLEDGMENTS

APPENDIX A: MEDIUM INTEGRALS

This section gives some details of the calculation of the loop integral for the full in-medium dimer-propagator. The loop integral $I(P_0,\mathbf{P})$ is defined as follows:

$$iI(P_0,\mathbf{P}) = \int_{|\mathbf{q}|<\Lambda} \frac{d^4q}{(2\pi)^4} \frac{i\Theta(|\frac{\mathbf{P}}{2}+\mathbf{q}|-k_F)}{\frac{P_0}{2}+q_0-\frac{1}{2}(\frac{\mathbf{P}}{2}+\mathbf{q})^2+i\epsilon}$$
$$\times \frac{i\Theta(|\frac{\mathbf{P}}{2}-\mathbf{q}|-k_F)}{\frac{P_0}{2}-q_0-\frac{1}{2}(\frac{\mathbf{P}}{2}-\mathbf{q})^2+i\epsilon}. \quad (A1)$$

After a contour integration the integral simplifies to

$$iI(P_0,\mathbf{P})$$
$$= i\int_{|\mathbf{q}|<\Lambda} \frac{d^3q}{(2\pi)^3} \frac{\Theta(|\frac{\mathbf{P}}{2}+\mathbf{q}|-k_F)\Theta(|\frac{\mathbf{P}}{2}-\mathbf{q}|-k_F)}{P_0-\frac{P^2}{4}-q^2+i\epsilon}. \quad (A2)$$

As already mentioned, the θ functions are boundary conditions to the integral. We choose $\mathbf{P}$ to be aligned in the z direction and switch to spherical coordinates. The ϕ integration still gives 2π. But the lower q boundary depends on θ, the angle between $\mathbf{P}$ and $\mathbf{q}$. The two θ functions are equivalent to the following conditions:

$$f^-(q) := q^2 - Pqx + \tfrac{1}{4}P^2 - k_F^2 > 0, \quad (A3)$$

$$f^+(q) := q^2 + Pqx + \tfrac{1}{4}P^2 - k_F^2 > 0, \quad (A4)$$

where $x = \cos\theta = \mathbf{Pq}/(Pq)$. The functions $f^\pm(q)$ are simple parabolas, whose roots are

$$f^+: \quad -\frac{Px}{2} \pm \sqrt{\frac{P^2}{4}(x^2-1)+k_F^2}, \quad (A5)$$

$$f^-: \quad +\frac{Px}{2} \pm \sqrt{\frac{P^2}{4}(x^2-1)+k_F^2}. \quad (A6)$$

These roots do only exist for all $x \in [-1,1]$ if $\frac{P}{2} \leqslant k_F$. Therefore, we have to distinguish the two cases $P > 2k_F$ and $P < 2k_F$.

(a) $P < 2k_F$: The θ functions move the lower boundary $a(x)$, which is

$$a(x) = \begin{cases} \frac{Px}{2} + \sqrt{\frac{P^2}{4}(x^2-1)+k_F^2} & \text{for } x > 0 \\ -\frac{Px}{2} + \sqrt{\frac{P^2}{4}(x^2-1)+k_F^2} & \text{for } x < 0 \end{cases}. \quad (A7)$$

The upper boundary remains unchanged. After a rescaling, $\frac{P}{2} = sk_F$, $q = tk_F$, $\widetilde{\Lambda} = \Lambda/k_F$ and $b = (P_0 - \frac{P^2}{4} + i\epsilon)/k_F^2$, the integral can be written as

$$iI(P_0,\mathbf{P}) = \frac{ik_F}{(2\pi)^2}\left\{ \int_0^1 \int_{sx+\sqrt{s^2(x^2-1)+1}}^{\tilde{\Lambda}} \frac{t^2}{b-t^2} \, dt \, dx \right. \quad (A8)$$

$$\left. + \int_{-1}^0 \int_{-sx+\sqrt{s^2(x^2-1)+1}}^{\tilde{\Lambda}} \frac{t^2}{b-t^2} \, dt \, dx \right\}. \quad (A9)$$

One can easily see that the second integral merges to the first if the substitution $x \to -x$ is performed.

(b) $P > 2k_F$: In this case the q integration range is

$$
\begin{cases}
\left[0, \frac{Px}{2} - \sqrt{c(x)}\right] \text{ and } \left[\frac{Px}{2} + \sqrt{c(x)}, \Lambda\right] & \text{for } \sqrt{1 - \frac{1}{s^2}} < x \leqslant 1 \\
[0, \Lambda] & \text{for } -\sqrt{1 - \frac{1}{s^2}} < x < \sqrt{1 - \frac{1}{s^2}} \\
\left[0, -\frac{Px}{2} - \sqrt{c(x)}\right] \text{ and } \left[-\frac{Px}{2} + \sqrt{c(x)}, \Lambda\right] & \text{for } -1 \leqslant x < -\sqrt{1 - \frac{1}{s^2}}
\end{cases}
$$

with $\sqrt{c(x)} := \sqrt{k_F^2 - \frac{P^2}{4}(1 - x^2)}$. Therefore, the integral becomes

$$
iI(P_0, P) = \frac{ik_F}{(2\pi)^2} \Biggl\{ \int_{-1}^{-\sqrt{1 - \frac{1}{s^2}}} \left(\int_0^{-sx - \sqrt{c'(x)}} \frac{t^2}{b - t^2} dt + \int_{-sx + \sqrt{c'(x)}}^{\tilde{\Lambda}} \frac{t^2}{b - t^2} dt \right) dx + \int_{-\sqrt{1 - \frac{1}{s^2}}}^{\sqrt{1 - \frac{1}{s^2}}} \int_0^{\tilde{\Lambda}} \frac{t^2}{b - t^2} \, dt \, dx
$$

$$
+ \int_{\sqrt{1 - \frac{1}{s^2}}}^1 \left(\int_0^{sx - \sqrt{c'(x)}} \frac{t^2}{b - t^2} dt + \int_{sx + \sqrt{c'(x)}}^{\tilde{\Lambda}} \frac{t^2}{b - t^2} dt \right) dx \Biggr\},
\tag{A10}
$$

with $c'(x) = 1 - s^2(1 - x^2)$. The integrals in the first and third line are equal, similiarly to the preceding case.

APPENDIX B: INTEGRAL KERNEL

In this section, we discuss the calculation of the integral

$$
\int_{-1}^1 d\cos\theta_q \, P_l(\cos\theta_q) \, t_{ik}(p, q, \theta_q, E)
\tag{B1}
$$

with

$$
t_{ij}(p, q, \theta_q, E) := \frac{\theta(|\mathbf{p} + \mathbf{q}| - k_F)(1 - \delta_{ij})}{E - p^2 - q^2 - pq\cos\theta_q + i\epsilon},
\tag{B2}
$$

which is required to derive the integral equation for the three-body amplitudes in the medium. This type of integral appears in the inhomgeneous as well as in the homgeneous part. The θ function is a boundary condition on the $\cos\theta_q$ integration:

$$
\theta(|\mathbf{p} + \mathbf{q}| - k_F) \Rightarrow p^2 + 2pq\cos\theta_q + q^2 > k_F^2.
\tag{B3}
$$

Two cases have to be distinguished. First, if $|p - q|$ is larger than k_F, the θ function is always fulfilled. Consequently, the integration region is $[-1, 1]$. If $|p - q| < k_F$, the lower boundary will be changed. Note that the q integration begins at k_F. The lower boundary θ_g is

$$
\cos\theta_g = \frac{k_F^2 - p^2 - q^2}{2pq}.
\tag{B4}
$$

The angle integration for the S wave can now be written

$$
\int_a^1 dx \frac{P_0(x)}{E - p^2 - q^2 - pqx + i\epsilon} = \frac{1}{pq} \int_a^1 dx \frac{1}{c - x} = -\frac{1}{pq} \left[\ln(c - x)\right]_a^1,
\tag{B5}
$$

with $c = \frac{1}{pq}(E - p^2 - q^2 + i\epsilon)$. The result is

$|p - q| > k_F : a = -1$

$$
-\frac{1}{pq}\left[\ln(c - x)\right]_a^1 = \frac{1}{pq}\left[\ln\left(\frac{E - p^2 - q^2 + pq + i\epsilon}{pq}\right) - \ln\left(\frac{E - p^2 - q^2 - pq + i\epsilon}{pq}\right)\right],
\tag{B6}
$$

$|p - q| < k_F : a = \cos\theta_g$

$$
-\frac{1}{pq}\left[\ln(c - x)\right]_a^1 = \frac{1}{pq}\left[\ln\left(\frac{E - \frac{1}{2}p^2 - \frac{1}{2}q^2 - \frac{1}{2}k_F^2 + i\epsilon}{pq}\right) - \ln\left(\frac{E - p^2 - q^2 - pq + i\epsilon}{pq}\right)\right].
\tag{B7}
$$

[1] S. Giorgini, L. P. Pitaevskii, and S. Stringari, Rev. Mod. Phys. **80**, 1215 (2008).

[2] W. Ketterle and M. Zwierlein, in *Proceedings of the International School of Physics "Enrico Fermi,"* Course CLXIV, edited by M. Inguscio, W. Ketterle, and C. Salomon (IOS Press, Amsterdam, 2008).

[3] D. Lee, Prog. Part. Nucl. Phys. **63**, 117 (2009).

[4] C. Chin, R. Grimm, P. Julienne, and E. Tiesinga, Rev. Mod. Phys. **82**, 1225 (2010).

[5] S. Tan, Ann. Phys. **323**, 2952 (2008); **323**, 2971 (2008); **323**, 2987 (2008).

[6] E. Braaten, Lect. Notes Phys. **836**, 193 (2012).

[7] V. Efimov, Phys. Lett. B **33**, 563 (1970).

[8] T. B. Ottenstein, T. Lompe, M. Kohnen, A. N. Wenz, and S. Jochim, Phys. Rev. Lett. **101**, 203202 (2008).

[9] J. H. Huckans, J. R. Williams, E. L. Hazlett, R. W. Stites, and K. M. O'Hara, Phys. Rev. Lett. **102**, 165302 (2009).

[10] E. Braaten, H.-W. Hammer, D. Kang, and L. Platter, Phys. Rev. Lett. **103**, 073202 (2009).

[11] S. Floerchinger, R. Schmidt, and C. Wetterich, Phys. Rev. A **79**, 053633 (2009).

[12] P. Naidon and M. Ueda, Phys. Rev. Lett. **103**, 073203 (2009).

[13] E. Braaten, H.-W. Hammer, D. Kang, and L. Platter, Phys. Rev. A **81**, 013605 (2010).

[14] T. Lompe, T. B. Ottenstein, F. Serwane, A. N. Wenz, G. Zürn, and S. Jochim, Science **330**, 940 (2010).

[15] S. Nakajima, M. Horikoshi, T. Mukaiyama, P. Naidon, and M. Ueda, Phys. Rev. Lett. **106**, 143201 (2011).

[16] T. Paananen, J.-P. Martikainen, and P. Törmä, Phys. Rev. A **73**, 053606 (2006).

[17] P. F. Bedaque and J. P. D'Incao, Ann. Phys. **324**, 1763 (2009).

[18] B. Errea, J. Dukelsky, and G. Ortiz, Phys. Rev. A **79**, 051603 (2009).

[19] G. Catelani and E. A. Yuzbashyan, Phys. Rev. A **78**, 033615 (2008).

[20] T. Ozawa and G. Baym, Phys. Rev. A **82**, 063615 (2010).

[21] A. Rapp, G. Zarand, C. Honerkamp, and W. Hofstetter, Phys. Rev. Lett. **98**, 160405 (2007).

[22] D. J. MacNeill and F. Zhou, Phys. Rev. Lett. **106**, 145301 (2011).

[23] N. G. Nygaard and N. T. Zinner, arXiv:1110.5854 [cond-mat.quant-gas].

[24] A. Storozhenko, P. Schuck, T. Suzuki, H. Yabu, and J. Dukelsky, Phys. Rev. A **71**, 063617 (2005); X. Barillier-Pertuisel, S. Pittel, L. Pollet, and P. Schuck, *ibid*. **77**, 012115 (2008); T. Watanabe, T. Suzuki, and P. Schuck, *ibid*. **78**, 033601 (2008).

[25] H.-W. Hammer and R. J. Furnstahl, Nucl. Phys. A **678**, 277 (2000).

[26] R. J. Furnstahl, G. Rupak, and T. Schafer, Annu. Rev. Nucl. Part. Sci. **58**, 1 (2008).

[27] J. V. Steele, arXiv:nucl-th/0010066.

[28] T. Schafer, C.-W. Kao, and S. R. Cotanch, Nucl. Phys. A **762**, 82 (2005).

[29] H.-W. Hammer and T. Mehen, Nucl. Phys. A **690**, 535 (2001).

[30] E. Braaten and H.-W. Hammer, Phys. Rep. **428**, 259 (2006).

[31] A. L. Fetter and J. D. Walecka, *Quantum Theory of Many-Particle Systems* (Dover, New York, 2003).

[32] E. Braaten, H.-W. Hammer, and M. Kusunoki, Phys. Rev. A **67**, 022505 (2003).

[33] P. F. Bedaque, H.-W. Hammer, and U. van Kolck, Phys. Rev. Lett. **82**, 463 (1999).

[34] Patrick Niemann, Diploma thesis, Universität Bonn, 2010.

[35] S. K. Adhikari, T. Frederico, Eur. Phys. J. B **5**, 219 (1998).

[36] T. Mehen, I. W. Stewart, and M. B. Wise, Phys. Rev. Lett. **83**, 931 (1999).

[37] S. Floerchinger, R. Schmidt, S. Moroz, and C. Wetterich, Phys. Rev. A **79**, 013603 (2009).